THE ASTROPHYSICAL JOURNAL, 466:L13–L16, 1996 July 20

ORTHOGONAL ROTATING GASEOUS DISKS NEAR THE NUCLEUS OF NGC 253

K. R. ANANTHARAMAIAH
Raman Research Institute, Bangalore 560 080, India

AND

W. M. GOSS
National Radio Astronomy Observatory, Socorro, NM 87801
Received 1996 January 2; accepted 1996 May 7

ABSTRACT

The central ~150 pc region of the starburst galaxy NGC 253 is shown to have a distinct gaseous kinematic subsystem, exhibiting rotation in a plane perpendicular to the galactic disk, and an interior region with possible counterrotation in the plane of the disk. In addition, solid-body rotation in the same sense as the galactic disk is observed in the outer parts of the central region. We suggest that this kinematic subsystem in NGC 253 may be indicative of a secondary bar inside the known primary bar. Alternatively, it may be a signature of a merger or an accretion event during the history of the galaxy. The dynamical mass within a radius of 5″ is $\sim 3 \times 10^8\ M_\odot$. These results are based on a two-dimensional image of the velocity field of the H92α recombination line in the central 9″ × 4″ region, with an angular resolution of 1.″8 × 1.″0, made using observations in the B, C, and D configurations of the VLA.

Subject headings: galaxies: individual (NGC 253) — galaxies: kinematics and dynamics — galaxies: starburst — radio lines: galaxies

1. INTRODUCTION

The velocity field in the nuclear starburst region of the Sc galaxy NGC 253, located in the Sculptor group, has been a subject of many studies in the optical, IR, and radio bands (Puxley & Brand 1995, and references therein). The measured Hα radial velocities along various position angles near the nucleus of NGC 253 show that, in addition to solid body rotation in the central region, there are large noncircular motions. These anomalous motions may indicate gas flowing out of the nucleus (Demoulin & Burbidge 1970; Ulrich 1978), possibly driven along the walls of a hollow cone by a massive starburst wind (Shulz & Wegner 1992) or by the joint action of several coeval detached star-forming centers (Muñoz-Tuñon, Vilchez, & Castañeda 1993). However, the large inclination of the plane of the galaxy to the line of sight (79°) and its attendant problems of obscuration at optical wavelengths seem to have weakened some of these deductions. At longer wavelengths, where obscuration is much less or absent, the measured radial velocities along the major axis seem to indicate only solid-body rotation in the central region (Canzian, Mundy, & Scoville 1988; Puxley & Brand 1995). These authors suggest that the measured optical velocities may correspond to foreground ionized gas, and, therefore, they may not represent the kinematics in the nuclear starburst region.

Radio recombination lines (RRL), which do not suffer from obscuration, provide an alternative method of studying kinematics in the nuclear region. NGC 253 is one of the relatively strong RRL sources, with a peak H92α ($\nu_{\rm rest}$ = 8.309 GHz) line flux density of about 8 mJy, with most of the line emission arising in the nuclear region (Anantharamaiah & Goss 1990). We have now observed this line, using the VLA, with an angular resolution of 1.″8 × 1.″0 (P.A. = 10°) and an rms noise of ~60 μJy beam^{-1}. The two-dimensional velocity field of the ionized gas in the central region shows a systematic S-shaped pattern, which is distinct from the larger scale velocity field of the outer disk. This is interpreted as evidence for three distinct rotations in the central region—a solid-body rotation in the same sense as the outer galaxy, a rotation in a perpendicular plane with almost twice the speed, and, finally, a possible counterrotating inner core. Thus, NGC 253 becomes the first nuclear starburst galaxy to exhibit a gaseous kinematic subsystem in its interior region. In this Letter, we adopt a distance to NGC 253 of 3.4 Mpc, which translates to a linear scale of 16.5 pc arcsec^{-1}.

2. OBSERVATIONS

In each of the three VLA configurations (B, C, and D), observations were made using 32 spectral channels with a total bandwidth of 25 MHz, corresponding to a velocity coverage of ~850 km s^{-1}, centered at a heliocentric velocity of 200 km s^{-1}. After Hanning smoothing, the resulting velocity resolution was 56.4 km s^{-1}. The total duration of the observations, made in several sessions between 1987 and 1990, was ~40 hr. Some preliminary results were published in Anantharamaiah & Goss (1990). All the data were processed again using the AIPS software package developed by NRAO.[1] The three databases were self-calibrated and combined into a single large data base. Continuum was subtracted from each visibility measurement by fitting a linear function through the spectral channels that were devoid of line emission. A line data cube was made of the visibilities with a "natural" weighting function. The images were deconvolved using the "clean" algorithm.

The H92α line image integrated over velocity is shown in Figure 1*a*. The distribution of central velocities, obtained by fitting a Gaussian profile at each pixel, is shown in Figure 1*b*. The similarity of Figure 1*a* to the observed continuum struc-

[1] The National Radio Astronomy Observatory is a facility of the National Science Foundation operated under a cooperative agreement by Associated Universities, Inc.

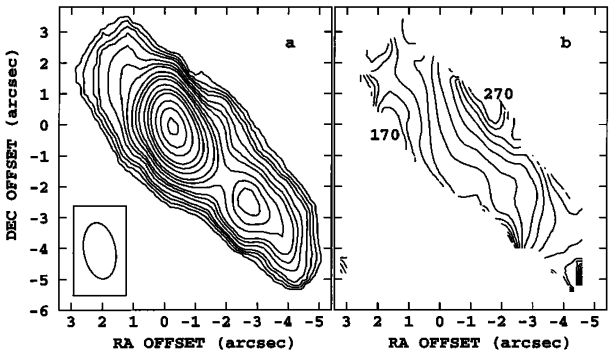

FIG. 1.—(*a*) Integrated H92α line emission from NGC 253. First contour and contour intervals are 7 Jy beam^{-1} m s^{-1}. Intervals double at contour numbers 4, 7, 10, and 13. (*b*) Velocity field from Gaussian fits. Contours are 170–270 in steps of 10 km s^{-1}. The offsets are with respect to $00^h45^m5\overset{s}{.}80$, $-25°33'39\overset{''}{.}1$ (B1950).

ture in the central region (e.g., Ulvestad & Antonucchi 1994) has important implications for the mechanism of line emission, which will be discussed in a further publication. The main subject for this Letter is the velocity field shown in Figure 1*b*, which concerns the motion of ionized gas in the central 150 × 60 pc region of NGC 253. The mean width of the lines (FWHM) is about 200 km s^{-1}, and the central velocity of the integrated line profile is 220 km s^{-1}.

3. KINEMATICS OF THE IONIZED GAS

An unusual aspect of the velocity distribution shown in Figure 1*b* is that the isovelocity contours in the nuclear region run roughly parallel to the major axis, and they have an overall stretched S shape. For solid-body rotation in the plane of the galaxy, which is typically found in the central regions of disk galaxies, the isovelocity contours are expected to run parallel to the minor axis. In Figure 2*a*, we show the central velocities along the major and minor axes obtained from the Gaussian fits. Pronounced velocity gradients of ~11 km s^{-1} arcsec^{-1} along the major axis and ~18 km s^{-1} arcsec^{-1} along the minor axis are observed. The velocity curve along the major axis is noteworthy since it displays a semisinusoidal pattern superposed on a linear gradient. The dashed curve in Figure 2*a*, which has a slightly higher angular resolution ($1\overset{''}{.}6 \times 0\overset{''}{.}9$) that was obtained using only the B-configuration data, shows that the sense of the velocity gradient reverses in the central 2″ region. These data show that in addition to solid-body rotation in the plane of the galaxy, other organized motions are present in the central 150 pc region of NGC 253.

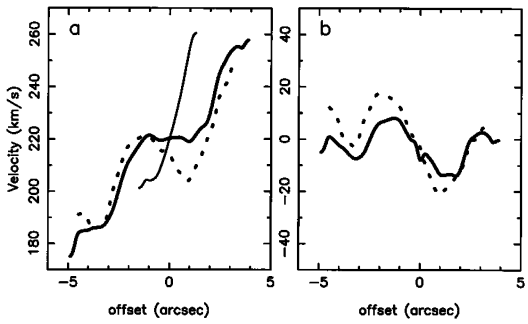

FIG. 2.—(*a*) H92α velocities along the major (*thick line*) and minor (*thin line*) axes. (*b*) Residual major-axis velocities after removing a gradient. Dotted lines are velocities from higher resolution data ($1\overset{''}{.}6 \times 0\overset{''}{.}9$). The offsets are with respect to $00^h45^m5\overset{s}{.}68$, $-25°33'40\overset{''}{.}3$ (B1950).

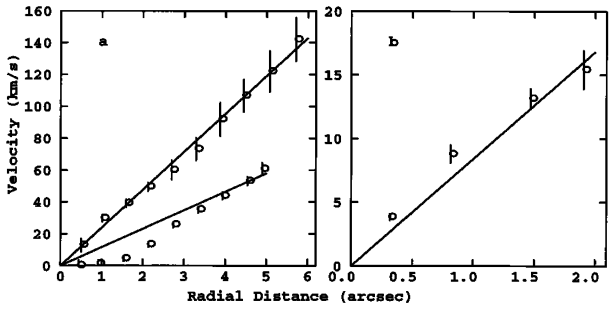

FIG. 3.—Fitted rotation curves for (*a*) minor-axis (*upper line*) and major-axis (*lower line*) rotations, and (*b*) major-axis counter-rotation. The reference position is the same as in Fig. 2.

We have compared the measured H92α velocity along the major axis with the velocities measured in Hα and [N II] (Ulrich 1978; Muñoz-Tuñon et al. 1993), CO (Canzian et al. 1988), and Brγ (Puxley & Brand 1995). The H92α measurements cover only a ~10″ region close to the nucleus, whereas the other measurements extend over a larger region (up to 100″). In the region of overlap, the mean H92α velocity and the velocity gradient are most consistent with the CO and Brγ data. The H92α velocities are less consistent with the optical observations of Ulrich (1978; the gradients are different) and completely inconsistent with the optical data of Muñoz-Tuñon et al. (1993). The inconsistency between optical and longer wavelength measurements must be a result of extinction, as noted by Canzian et al. (1988) and Puxely & Brand (1995). Hence, some of the conclusions regarding noncircular motions derived from optical studies should apply to foreground gas rather than to the nuclear region of NGC 253. The agreement in velocity between H92α, CO, and Brγ indicates that the ionized gas observed in H92α is located in the nuclear region of NGC 253.

3.1. *A Model of Perpendicular and Counterrotating Rings*

Based on the velocity pattern (Fig. 1*b*), a motion, which is roughly perpendicular to plane of the galaxy, must dominate the velocity field in the central region. First, we attempted to fit a solid-body rotation model to the velocity field in Figure 1*b*, using the procedure GAL provided in the AIPS software package. The inclination angle of the galaxy was held fixed at $i = 78.5°$ (Pence 1981). After trying several positions near the emission peak, the optimum center of the velocity field (i.e., the dynamical center) was found to be $(\alpha, \delta)_{1950} = 00^h45^m5\overset{s}{.}68$, $-25°33'40\overset{''}{.}3$ (1 σ error $\sim 0\overset{''}{.}3$), which is $\sim 1\overset{''}{.}8$ southwest of the H92α line peak in Figure 1*a*. The procedure GAL computes the circular velocity in a series of annuli, and it makes a least-squares fit in order to obtain the systemic velocity, the rotation curve, and the position angle. The fitted systemic velocity is 227 ± 1 km s^{-1}. Solid-body rotation with a gradient of ~24 km s^{-1} gives an excellent fit to the circular velocities, as shown by the upper line in Figure 3*a*. *But the unusual aspect of this rotating solid body is that the position angle of its receding part is* 324° ± 4°, *which is almost exactly along the minor axis of the galaxy* (P.A. = 321°). The velocity field of this rotation is a set of isovelocity contours running parallel to the major axis, and the axis of rotation lies in the plane of the galaxy. Since the isovelocity contours in Figure 1*b* extend over 4″–5″ parallel to the major axis, this annular ring is either cylindrical in shape or it is a thin ring, which is not seen edge-on but inclined at some angle to the line of sight.

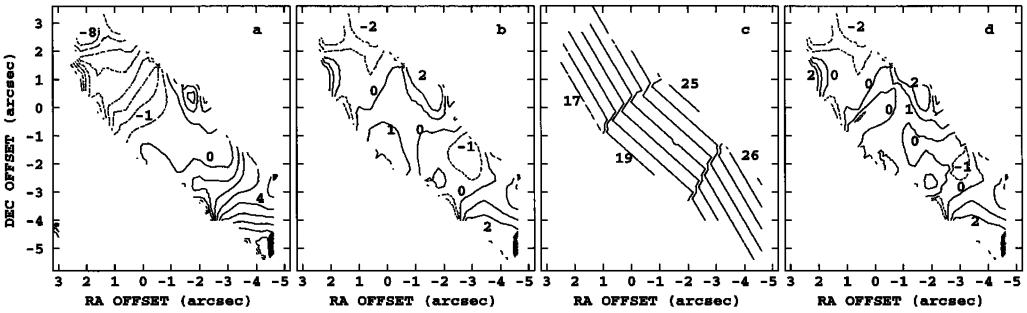

FIG. 4.—Residual velocity field (*a*) after removing minor-axis rotation and (*b*) after removing minor- and major-axis rotations. (*c*) Model velocity field. (*d*) Residual velocities after subtracting the model in (*c*) from the observed velocities shown in Fig. 1*b*. Contours are −80 to +80 km s^{-1} in (*a*), −20 to +20 km s^{-1} in (*b*) and (*d*), and 170–270 km s^{-1} in (*c*). Contour intervals are 10 km s^{-1}. Selected contours are labeled in units of 10 km s^{-1}. The reference position is same as in Fig. 1.

A subtraction of the velocity field of the above ring (which rotates in a plane orthogonal to the galactic disk) from the observed velocity field in Figure 1*b* produces the residuals shown in Figure 4*a*. These residuals *now reveal the familiar solid-body rotation in the plane of the galaxy*, which is likely to be just the continuation of the solid-body rotation observed on a larger scale of the nuclear region (Canzian et al. 1988). The isovelocity contours in Figure 4*a* (which run roughly parallel to the minor axis) do not extend all the way to the center, which indicates that the interior region (about 2″ in extent) may have yet another kind of motion.

The fitting procedure described above can again be applied to the residuals shown in Figure 4*a*, in order to obtain the rotation curve of the outer disk. The resulting fit is shown in Figure 3*a* (*lower line*). The velocity gradient is about 12 km s^{-1} arcsec^{-1}, and, as expected, the fitted position angle of the receding part of the solid body, 230° ± 5°, is close to the P.A. of the major axis (231°; Pence 1981). Figure 4*b* shows the residual velocity field obtained by subtracting this rotation model from the velocity field in Figure 4*a*. Although the magnitude of the residuals in Figure 4*b* are small (±10 km s^{-1}), a systematic pattern is present, especially in the inner few arcsecond region. As seen in Figure 3*a*, the major axis rotation curve gives a poor fit to the observed velocities very close to the nucleus, indicating that some other type of motion may still be present in the very inner region. This pattern is more clearly evident in Figure 2*b*, where we show the residual velocity along the major axis. The semisinusoidal pattern along the major axis (Fig. 2*a*) is still present in Figure 2*b*, although the gradient is removed by the above model. It is clear that the apparent sinusoidal pattern in Figure 2*b* is a result of insufficient angular resolution; there are only three to four independent points in the central ±2″ region. Plots of the major-axis velocity with slightly higher angular resolution (*dotted lines* in Fig. 2), clearly indicate that the sense of the velocity gradient reverses in the central 2″ region. This reversal of the gradient can be interpreted as indicating yet another rotation in the plane of the galaxy, *but in the opposite sense compared to the larger scale rotation*. A solid-body rotation, with a P.A. = 51° (i.e., major axis) fitted to the inner 0″–2″ region of the residuals in Figure 4*b*, gives the rotation curve shown in Figure 3*b*. The velocity gradient in this very central counterrotating core is ∼8 km s^{-1} arcsec^{-1}. The model velocity field obtained by combining all the three rotations is shown in Figure 4*c*, which roughly mimics the observed velocity field shown in Figure 1*b*. The final residuals obtained by subtraction of this model from the observed velocity field is shown in Figure 4*d*. The rms of these residuals, which are essentially random, is ∼5 km s^{-1}.

In summary, one possible model that can explain the observed velocity field shown in Figure 1*b* consists of three nested rings or disks of ionized gas rotating like solid bodies. The outermost ring, with a velocity gradient of 12 km s^{-1} arcsec^{-1}, rotates in the plane of the galaxy and is likely to be a part of the general solid-body rotation found near the center on larger scales (Pence 1981; Canzian et al. 1988; Puxley & Brand 1995). The second ring, which is interior to the outer disk, dominates the velocity field in the central region with a gradient of 24 km s^{-1} arcsec^{-1}, and it is oriented perpendicular to the outer disk and likely to be tilted with respected to the line of sight. It should be noted that the data only imply that the spin axis of this ring lies in the plane of the galaxy and need not necessarily be aligned with the projected major axis of the galaxy's outer disk. The third and the most interior disk, the evidence for which is tentative because of the coarse angular resolution, is in the plane of the galaxy and appears to be rotating counter to the outermost disk. The velocity gradient of the innermost disk is ∼8 km s^{-1} arcsec^{-1}. The highest velocity gradient—24 km s^{-1} arcsec^{-1}, observed for the minor-axis rotation (Fig. 3*a*) implies a dynamical mass of $\sim 3 \times 10^8$ $M_\odot$ within a radius of 80 pc from the nucleus, based on the assumption of circular rotation.

4. DISCUSSION

While the model presented above, with three rotating components in the nuclear region, provides a reasonable fit to the observed velocity field, other models involving rotation, outflow, or inflow of ionized gas or warped disks may be possible. We have not evaluated such models. For larger scales, comparable to the size of the galactic disks, warped-disk models are known to produce S-shaped isovelocity contours, as in the case of M83 (Rogstad, Lockhart, & Wright 1974) and NGC 5383 (Peterson et al. 1978). In some sense, our model above is qualitatively similar but with an extreme form of warp, in which the inner two rings are tilted with respect to the outer one by 90° and 180°.

The S-shaped velocity field of NGC 5383 has also been modeled by Roberts, Huntely, & Van Albada (1979) as owing to the presence of a bar potential, which produces isovelocity contours oriented parallel to the bar axis. Although NGC 253 also has a bar, its position angle is ∼68° (Scoville et al. 1985), whereas the isovelocity contours in Figure 1*b* are oriented parallel to the major axis at a position angle of ∼51°. Therefore, we consider it unlikely that the potential of this bar

has influenced the observed velocity field in Figure 1*b*. However, since some disk galaxies are known to have a secondary bar within a primary bar (Friedli & Martinet 1993) with a different position angle, it may be possible to explain the observed velocity structure by invoking such an interior secondary bar. Theoretical work by Tohline & Durisen (1982) has shown that if the potential in the interior region of a galaxy is dominated by a "tumbling" prolate spheroidal (barlike) component, then gas in the innermost region will align its angular momentum vector along the major axis of the bar, which may be in the plane of the galaxy. It is possible that the orthogonal rotating disk detected in NGC 253 is indicative of such a barlike component. We note here that the center of our Galaxy also exhibits a tilted rotating ring of ionized and neutral gas (Burton & Liszt 1978; Lacy et al. 1979), which may be understood in terms of a barred potential (Binney et al. 1991). The observed kinematics in the central region of NGC 253 may be a related phenomenon.

The main result of our modeling of the S-shaped velocity field is that the ionized gas in the central region of NGC 253 seems to form a kinematic subsystem, distinct from the main outer galaxy, consisting of two perpendicular rotations (the rotation in an orthogonal plane and the central counter rotation in the plane). This kinematic subsystem may not be unlike some systems found in several elliptical galaxies, which exhibit rotation about the major axis (Franx, Illingowrth, & Heckman 1989) and counterrotating stellar cores (see Bender 1990 for a review). In one case, a unique system of two large cospatial counterrotating stellar disks has been detected (Rubin, Graham, & Kenney 1992). Such distinct kinematic subsystems are yet rare in disk galaxies. Two cases are known to date. Historically, the first such system seems to be NGC 3672, an Sc galaxy that was found by Rubin, Thonnard, & Ford (1977) to have a nuclear gas disk with a rotation axis that is almost perpendicular to that of the outer stellar disk. A more spectacular case, that of the Sab galaxy NGC 4826, was found by Braun, Walterbos, & Kennicut (1992) to have a large (~2 kpc) counterrotating inner gaseous disk.

The origin of such distinct kinematic subsystems is thought to be some kind of a merger or an accretion event during the history of the galaxy (Barnes 1991; Schweizer 1993). In one such scenario, modeled numerically (Hernquist & Barnes 1991), it was found that merger of two gas-rich disk galaxies of equal mass and antiparallel spin results in a dense central core of gas, which counterrotates with respect to the main remnant. It has been postulated that continued star formation in such disks could lead to counterrotating stellar cores, observed in some elliptical galaxies. A merger model such as that of Hernquist & Barnes (1991), with different parameters for the galaxies and their encounter, may explain the kinematics of the central region of NGC 253. In addition to producing kinematic subsystems, mergers of disk galaxies are also known to induce nuclear starbursts (Joseph 1990; Barnes 1991) leading to some of the most powerful infrared galaxies (Joseph & Wright 1985). Since NGC 253 is an archetypal nuclear starburst galaxy and is now shown to have a distinct kinematic subsystem in its nuclear region, we may be simultaneously witnessing two signatures of a past merger or an accretion event in this galaxy. Thus, NGC 253 may represent an intermediate stage of the merger process. Since there are no obvious signatures of an ongoing or a completed merger process in NGC 253, such as tidal "tails" or distortions in the disk, the event probably involved a relatively small companion that was accreted onto a large disk galaxy.

Kinematic subsystems in disk galaxies (found so far only in NGC 3672, NGC 4826, and NGC 253) appear to be relatively rare compared to ellipticals in which more than a dozen or so cases are known. This could be owing to an observational selection effect. Intense nuclear starburst systems, such as NGC 253, have large extinctions in the nuclear region at optical wavelengths. As a result, unless the kinematic subsystems in disk galaxies extend to large radii, as in the case of NGC 4826, and are not confined to the central core as in NGC 253, their signatures may be missed in optical spectroscopic studies. This problem of obscuration seems to have occurred in the case of NGC 253. Although many optical spectroscopic studies, beginning with that of Demoulin & Burbidge (1970), recognized the existence of noncircular motion in the central region, they failed to uncover the very systematic velocity pattern observed here in the H92α line. The surprise discovery of a kinematically distinct core in this previously well-studied starburst galaxy suggests that measurements of two-dimensional velocity fields of the central regions of other starburst galaxies with high angular resolution, at a wavelength free of obscuration, may lead to more discoveries of fascinating kinematic substructures.

REFERENCES

Anantharamaiah, K. R., & Goss, W. M. 1990, in IAU Colloq. 125, Radio Recombination Lines: 25 Years of Investigations, ed. M. A. Gordon & R. L. Sorochenko (Dordrecht: Kluwer), 267
Barnes, J. E. 1991, in IAU Symp. 146, Dynamics of Galaxies and Their Molecular Cloud Distributions, ed. F. Combes & F. Casoli (Dordrecht: Kluwer), 363
Bender, R. 1990, in Dynamics and Interactions of Galaxies, ed. R. Wielen (Berlin: Springer), 232
Binney, J., Gerhard, O. E., Stark, A. A., Bally, J., & Uchida, K. I. 1991, MNRAS, 252, 210
Braun, R., Walterbos, R. A. M., & Kennicut, R. C. 1992, Nature, 360, 442
Burton, W. B., & Liszt, H. S. 1978, ApJ, 225, 815
Canzian, B., Mundy, L. G., & Scoville, N. Z. 1988, ApJ, 333, 157
Demoulin, M.-H., & Burbidge, E. M. 1970, ApJ, 159, 799
Franx, M., Illingworth, G., & Heckman T. 1989, ApJ, 344, 613
Friedli, D., & Martinet, L. 1993, in Physics of Nearby Galaxies: Nature or Nurture?, ed. T. X. Thuan, C. Balkowski, & J. T. Thanh Van (Gif-sur-Yvette: Editions Frontières), 527
Hernquist, L. E., & Barnes, J. E. 1991, Nature, 354, 210
Joseph, R. D. 1990, in Dynamics and Interactions of Galaxies, ed. R. Wielen (Berlin: Springer), 132
Joseph, R. D., & Wright, G. S. 1985, MNRAS, 214, 87
Lacy, J. H., Baas, F., Townes, C. H., & Geballe, T. R. 1979, ApJ, 227, L17
Muñoz-Tuñon, C., Vilchez, J. M., & Castañeda, H. O. 1993, A&A, 278, 364
Pence, W. D. 1981, ApJ, 247, 473
Peterson, C. J., Rubin, V. C., Ford, W. K., & Thonnard, N. 1978, ApJ, 219, 31
Puxley, P. J., & Brand, P. W. J. L. 1995, MNRAS, 274, L77
Roberts, W. W., Huntely, J. M., & Van Albada, G. D. 1979, ApJ, 233, 67
Rogstad, D. H., Lockhart, I. A., & Wright, M. C. H. 1974, ApJ, 193, 309
Rubin, V. C., Graham, J. A., & Kenny, J. D. P. 1992, ApJ, 394, L9
Rubin, V. C., Thonnard, N., & Ford, W. K. 1977, ApJ, 217, L1
Schweizer, F. 1993, in Physics of Nearby Galaxies: Nature or Nurture?, ed. T. X. Thuan, C. Balkowski, & J. T. Thanh Van (Gif-sur-Yvette: Editions Frontières), 283
Scoville, N. Z., Soifer, B. T., Neugebauer, G., Young, J. S., Mathews, K., & Yerka, J. 1985, ApJ, 289, 129
Shulz, H., & Wegner, G. 1992, A&A, 266, 167
Tohline, J. E., & Durisen, R. H. 1982, ApJ, 257, 94
Ulrich, M.-H. 1978, ApJ, 219, 424
Ulvestad, J. S., & Antonucci, R. R. J. 1994, ApJ, 424, L29